Caveolin-1 alters Ca^{2+} signal duration through specific interaction with the $G\alpha_q$ family of G proteins

Parijat Sengupta, Finly Philip* and Suzanne Scarlata‡

Department of Physiology and Biophysics, BST6-145, Stony Brook University, Stony Brook, NY 11794-8661, USA
*Present address: Department of Pharmacology, University of Texas Southwestern at Dallas, Dallas, TX, USA
‡Author for correspondence (e-mail: Suzanne.Scarlata@sunysb.edu)

Accepted 28 January 2008
Journal of Cell Science 121, 1363-1372 Published by The Company of Biologists 2008
doi:10.1242/jcs.020081

Summary

Caveolae are membrane domains having caveolin-1 (Cav1) as their main structural component. Here, we determined whether Cav1 affects Ca^{2+} signaling through the $G\alpha_q$–phospholipase-Cβ (PLCβ) pathway using Fischer rat thyroid cells that lack Cav1 ($FRTcav^-$) and a sister line that forms caveolae-like domains due to stable transfection with Cav1 ($FRTcav^+$). In the resting state, we found that eCFP-Gβγ and $G\alpha_q$-eYFP are similarly associated in both cell lines by Forster resonance energy transfer (FRET). Upon stimulation, the amount of FRET between $G\alpha_q$-eYFP and eCFP-Gβγ remains high in $FRTcav^-$ cells, but decreases almost completely in $FRTcav^+$ cells, suggesting that Cav1 is increasing the separation between $G\alpha_q$-Gβγ subunits. In $FRTcav^-$ cells overexpressing PLCβ, a rapid recovery of Ca^{2+} is observed after stimulation. However, $FRTcav^+$ cells show a sustained level of elevated Ca^{2+}. FRET and colocalization show specific interactions between $G\alpha_q$ and Cav1 that increase upon stimulation. Fluorescence correlation spectroscopy studies show that the mobility of $G\alpha_q$-eGFP is unaffected by activation in either cell type. The mobility of eGFP-Gβγ remains slow in $FRTcav^-$ cells but increases in $FRTcav^+$ cells. Together, our data suggest that, upon stimulation, $G\alpha_q$(GTP) switches from having strong interactions with Gβγ to Cav1, thereby releasing Gβγ. This prolongs the recombination time for the heterotrimer, thus causing a sustained Ca^{2+} signal.

Key words: G proteins, Ca^{2+} signaling, Caveolin-1, Phospholipase C

Introduction

Caveolae are prominent protein domains in membranes that are believed to be involved in receptor desensitization, endocytosis, transcytosis, vesicle trafficking, cell migration and other cellular events (for reviews, see Anderson, 1998; Marx, 2001; Navarro et al., 2004; Okamoto et al., 1998; Ostrom and Insel, 2004; Parton and Simons, 2007; Schlegel et al., 1998). In many cell lines, caveolae are comprised largely of the protein caveolin-1 (Cav1), whereas caveolin-3 is the major component in skeletal, and in some types of smooth muscle cells. Cav1 contains multiple palmitoylation sites and forms tightly packed domains with membrane components that form lipids rafts, such as cholesterol and lipids with saturated hydrocarbon chains. The tight packing in these domains might promote the localization of proteins containing saturated hydrocarbon chains as opposed to ones that have unsaturated chains. Caveolae have been proposed to serve as nucleation sites that organize complexes of related signaling proteins through specific interactions with its scaffold domain (see Marx, 2001). Support of this idea comes from cell fractionation studies, which have identified several types of G-protein-coupled receptors (GPCRs) as well as their corresponding Gα subunits in caveolae fractions (Liu et al., 2002; Ostrom and Insel, 2004). Additionally, caveolae will sequester and internalize a select group of GPCRs during desensitization, although it is not clear whether internalization is accompanied by other mechanisms, such as through clathrin-coated pits. The underlying basis for caveolae-mediated as opposed to clathrin-mediated endocytosis is not clear, and it is also unclear whether internalization mechanisms are different in cell lines that do not contain caveolae.

In this study, we focused on the role of Cav1 in organizing proteins involved in the muscarinic-receptor–$G\alpha_q$–Gβγ–phospholipase-Cβ signaling system. This pathway can be activated by acetylcholine, or by its stable analog carbachol, to promote the activation of phospholipase Cβ (PLCβ) by activated $G\alpha_q$ in the case of PLCβ isozymes 1-4 and additionally by Gβγ for PLCβ isozymes 2 and 3. PLCβs catalyze the hydrolysis of a minor component in lipid membranes – phosphatidylinositol (4,5)-bisphosphate: [PtdIns(4,5)P_2] – to produce two second messengers, inositol (1,4,5)-trisphosphate [Ins(1,4,5)P_3] and diacylglycerol (DAG). Ins(1,4,5)P_3 diffuses into the cytosol, where it induces release of Ca^{2+} from the Ins(1,4,5)P_3-sensitive Ca^{2+} storage compartments. In response to this increase in cytosolic Ca^{2+}, protein kinase C (PKC) migrates from the cytosol to the cell membrane, where it is activated by DAG (for reviews, see Rebecchi and Pentyala, 2000; Rhee, 2001). These changes, in turn, stimulate a host of proliferative and mitogenic changes in the cell.

There have been numerous studies regarding the ability of caveolae to sequester G proteins (e.g. deWeerd and Leeb-Lundberg, 1997; Li et al., 1995; Liu et al., 2002; Lockwich et al., 2000; Smart et al., 1995). However, the results of many of these studies have varied widely, most probably because they involve cell disruption and fractionation in order to partially isolate caveolae domains, and/or because different cell lines have been used (e.g. Schnitzer et al., 1995; Stan et al., 1997). Of note are studies that have found that $G\alpha_q$ proteins, but not other Gα families, reside in caveolae domains (Oh and Schnitzer, 2001), suggesting that caveolae might organize complexes between $G\alpha_q$ subunits and protein partners. In a previous study, we found that $G\alpha_q$-PLCβ complexes are stably associated both in the basal and carbachol-activated states in living PC12 and HEK293 cells (Dowal et al., 2006a), which both express Cav1. It is thus possible that Cav1 might stabilize the plasma membrane localization of $G\alpha_q$ and its associated proteins.

To determine whether Cav1 expression affects G-protein-subunit association in living cells, we compared the interaction between $G\alpha_q$ and $G\beta\gamma$ in wild-type Fisher rat thyroid (FRTcav$^-$) cells, which do not contain caveolae domains because of a lack of Cav1 expression, to a stable transfection line of FRT cells that express Cav1 and form caveolae-like domains (FRTcav$^+$) (see Lipardi et al., 1998). FRT cell lines contain muscarinic receptors (mostly the M_3 subtype) that couple to $G\alpha_q$, allowing us to monitor the behavior of $G\alpha_q$ in these cells upon carbachol activation (Jimenez et al., 2001). Previous studies have shown that expression of Cav1 in FRT cells does not affect the expression, sorting or localization of human folate receptors (Kim et al., 2002) or proteins involved in cholesterol trafficking (Wang et al., 2003). Similarly, we found here that Cav1 expression does not affect the expression or plasma membrane localization of overexpressed G-protein subunits.

Here, we monitored the interaction of $G\alpha_q$ and $G\beta\gamma$ in the two types of FRT cells by Forster resonance energy transfer (FRET) and fluorescence correlation spectroscopy (FCS) using proteins tagged with GFP and its variants. FRET measurements allow us to monitor protein-protein association on membrane surfaces of living cells in real time (e.g. Philip et al., 2007) and FCS measures the average mobility of cell surface proteins (e.g. Sengupta et al., 2002). We also performed a series of fluorescence-based in vitro studies and Ca^{2+}-release experiments. We found that Cav1 binds preferentially to $G\alpha_q$ in its activated state. This binding appears to hinder $G\alpha_q$ interactions with $G\beta\gamma$ subunits that are required for signal termination, thus prolonging the activated state, as observed by a sustained presence of a higher level of Ca^{2+}. These results indicate that Cav1 might play a role in the duration of G-protein signals.

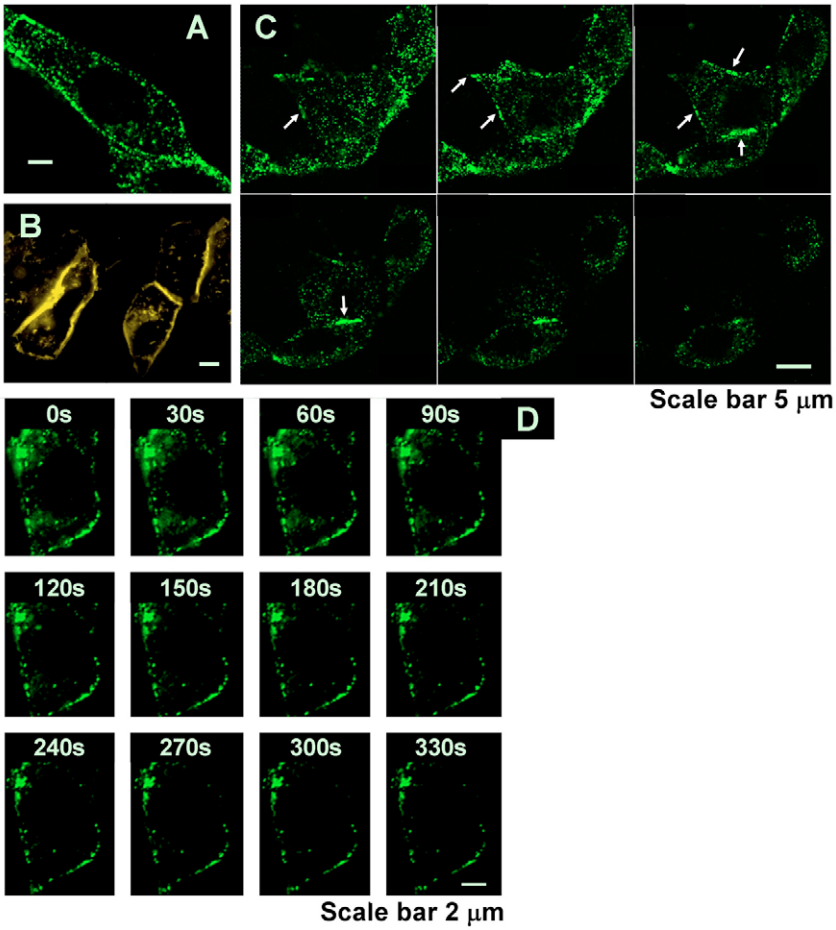

Fig. 1. Distribution of Cav1-eGFP in FRT cells in the basal and stimulated states. (A) Confocal image of an FRT cell expressing Cav1-eGFP, showing typical punctuate structures. (B) Confocal image of FRT cells expressing a membrane marker, MEM-eYFP, showing uniform distribution. (C) *z* stack of confocal images (from bottom to top) illustrate the cellular distribution of Cav1-eGFP in different planes of FRT cells. Cav1-eGFP forms large punctuate structures (indicated by white arrows) on the membrane. The thickness of each slice is 1 μm. Scale bar: 5 μm. (D) A time series of fluorescence images showing that stimulation of FRT cells expressing Cav1-eGFP does not cause internalization of Cav1-eGFP when muscarinic receptors are stimulated using 5 μM carbachol. Scale bar: 2 μm. Total duration of time series is 330 seconds.

Results

Distribution of Cav1 in basal-state and stimulated FRT cells

We transiently transfected Cav1-eGFP in FRTcav$^-$ cells at an efficiency above ~70%, and used confocal microscopy to confirm its cellular localization and distribution (Fig. 1). Cav1-eGFP was almost exclusively found on the plasma membrane. A cytosolic or Golgi population could only be seen in cells in which the expression level was very high. Although caveolae structures, which are typically 50-100 nm in length, are not in the appropriate range for resolution by light microscopy, we did find that a considerable fraction of Cav1-eGFP forms large patches or punctuate structures on the plasma membrane (Fig. 1A,C). These structures were often as large as 2 μm in size (length/diameter) and often located in the region of cell-cell junctions. A series of confocal images recorded over 45 minutes showed little movement of Cav1-eGFP structures (data not shown). Note that closely packed small (50-100 nm) structures on the plasma membrane will appear as a large structure when viewed under confocal microscope because the spatial resolution is limited by the wavelength of light used, which was 488 nm in this particular experiment. Nevertheless, Cav1-eGFP was entirely plasma membrane localized in a non-uniform distribution, indicating regions that exclude Cav1-eGFP. This pattern is in contrast to the uniform plasma membrane distribution seen for the commercial plasma membrane marker GFP-MEM (Clontech) (Fig. 1B). Immunofluorescence experiments using anti-Cav1 antibody showed similar punctuate distribution on the plasma membrane of FRTcav$^+$ cells (e.g. Mora et al., 1999) and Madin-Darby canine kidney (MDCK) cells (Mora et al., 1999). MDCK cells express high level of endogenous Cav1.

We stimulated FRTcav$^-$ cells expressing Cav1-eGFP with 5 μM carbachol and recorded a time series of images for ~10 minutes with a frame-acquisition rate of 12 frames/minute (Fig. 1D). We could not detect Cav1-eGFP internalization upon receptor activation. This result supports previous findings that muscarinic receptors mostly internalize via a clathrin-mediated pathway (Tobin, 1997) and indicates that, in FRT cells, Cav1 is not involved in M_3-receptor internalization.

Effect of Cav1 on the interaction between $G\alpha_q$ and $G\beta\gamma$ during signaling

We studied the effect of Cav1 expression on $G\alpha_q$-$G\beta\gamma$ association by monitoring FRET between eCFP-$G\beta\gamma$ and $G\alpha_q$-eYFP in basal and stimulated FRTcav$^-$ and FRTcav$^+$ cells. FRTcav$^+$ cells used in these experiments were stably transfected with Cav1. We found that both $G\alpha_q$-eYFP and eCFP-$G\beta\gamma$ subunits localized on the plasma membrane in FRTcav$^+$ and FRTcav$^-$ cells, indicating that stable expression of Cav1 in FRT cells does not alter the cellular localization of G-protein subunits. We expect a similar punctuate cellular distribution of Cav1 in FRTcav$^+$ cells as Cav1-eGFP in the transiently transfected FRTcav$^-$ cells shown in Fig. 1A,C.

For the eCFP-eYFP FRET pair, the distance at which the probability of energy transfer from donor to acceptor is 50% (i.e. R_0) is estimated to be 45-49 Å (Patterson et al., 2000). Because FRET efficiency is inversely proportional to the sixth power of the distance between donor (eCFP) and acceptor (eYFP), a small increase in intermolecular distance will significantly reduce the amount of FRET. Theoretical calculations show a complete loss of FRET between eCFP and eYFP above a separation of 100 Å (data not shown), although the signal will probably subside at shorter distances (see Lakowicz, 1999).

We first measured the FRET from negative and positive control samples. Two negative controls were used: (1) for eCFP and eYFP co-expressed in cells, a normalized FRET (N_{FRET}) value (see Materials and Methods) of 0.18±0.02 (n=12) was obtained (Fig. 2C); (2) for membrane-bound $G\alpha_i$-eCFP and eYFP-PLCδ1, the N_{FRET} value obtained was 0.15±0.02 (n=8). This value reflects stochastic non-specific encounters between freely diffusing proteins tagged either with eCFP or with eYFP in addition to the limitations imposed by the optical components in our FRET setup. These numbers represent the minimum detectable level of N_{FRET} in our instrument. The maximum level of FRET was determined using a positive control (eCFP and eYFP separated by an eight-amino-acid linker), which yielded an N_{FRET} value of 0.67±0.05 (n=11). Thus, the working range of normalized FRET (N_{FRET}) for our samples was ~0.70 and 0.20.

For eCFP-$G\beta\gamma$ and $G\alpha_q$-eYFP in either FRTcav$^-$ or FRTcav$^+$ cells, we obtained a similar value of normalized FRET (0.52±0.03; Fig. 2A,B) in the basal state. The value of FRET remained constant over 2 minutes in both cell types. Considering that we overexpressed the proteins at two- to three-fold above endogenous levels, as determined by western blot analysis using purified protein for comparison (F.P., unpublished), and that the fluorescent-tagged protein competes with endogenous protein for its partner, the high value of FRET suggests that a significant fraction of the G-protein subunits are associated in the basal state. We also note that the normalized FRET values in both cell lines were identical, suggesting that the presence of Cav1 does not affect the extent of $G\alpha_q$-$G\beta\gamma$ association in the basal state.

Upon cell stimulation with 5 μM acetylcholine, the normalized FRET from eCFP-$G\beta\gamma$ to $G\alpha_q$-eYFP increased from 0.52±0.03 to 0.76±0.05 within the first 20 seconds in both FRTcav$^-$ and FRTcav$^+$ cells (Fig. 2A,B). This increase has been previously observed for $G\alpha_i$-eYFP and eCFP-$G\beta\gamma$ with fluorescent tags attached at similar positions on the G-protein subunits, and has been interpreted as re-orientation of the subunits upon activation (see Bunemann et al., 2003).

In FRTcav$^-$ cells, the normalized FRET returned to the basal value ~1 minute after the initial increase (Fig. 2). By contrast, in FRTcav$^+$ cells, the initial increase was followed by a significant reduction to a value below our level of detection (i.e. less than 0.2). This large decrease in normalized FRET seen in FRTcav$^+$ cells, but not in FRTcav$^-$ cells, suggests that $G\alpha_q$-eYFP is separating from eCFP-$G\beta\gamma$ subunits in cells expressing Cav1.

We could not measure reassembly of $G\alpha_q$ and $G\beta\gamma$ after withdrawal of the agonist using FRET because preferential bleaching in CFP channel introduced errors too great for us to confidently report these results.

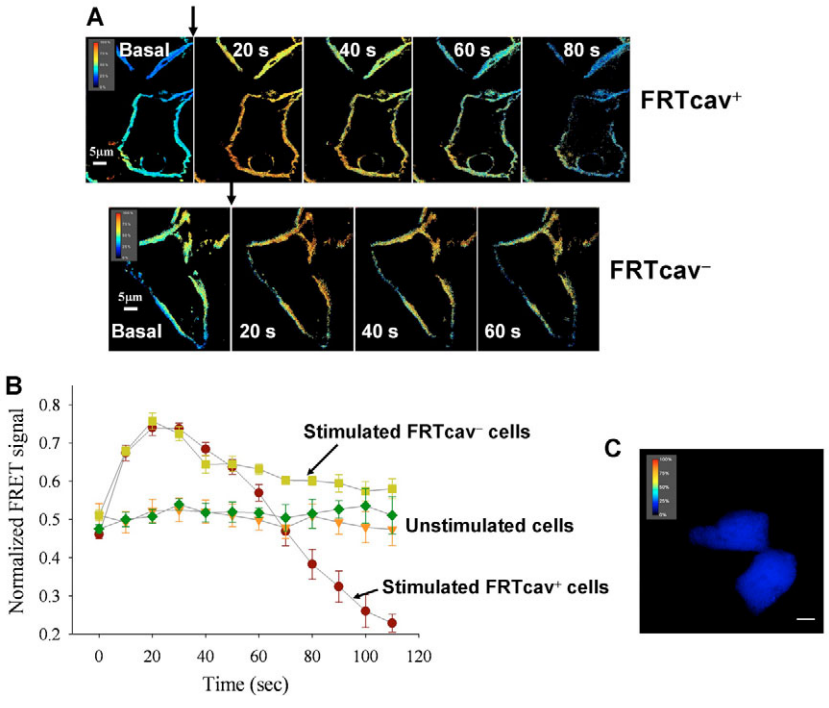

Fig. 2. $G\beta\gamma$ and $G\alpha_q$ subunits dissociate upon carbachol stimulation in the presence of Cav1. (A) Pseudo-colored FRET images illustrating the time-dependence of energy transfer from eCFP-$G\beta\gamma$ to $G\alpha_q$-eYFP in acetylcholine (5 μM)-stimulated FRTcav$^+$ (upper panel) and FRTcav$^-$ (lower panel) cells. The FRET color-scale is shown for comparison (red, 100%; black, 0%). For both series, the first panel was recorded before stimulation and the elapsed time between each image is 20 seconds. (B) Compiled results of the changes in N_{FRET} from eCFP-$G\beta\gamma$ to $G\alpha_q$-eYFP in unstimulated and acetylcholine (5 μM)-stimulated FRTcav$^+$ and FRTcav$^-$ cells with time. Studies were done using nine (FRTcav$^-$) and four (FRTcav$^+$) independent sets of samples (each measured in triplicate and averaged). (C) Pseudo-colored N_{FRET} image illustrating energy transfer between free eCFP and eYFP.

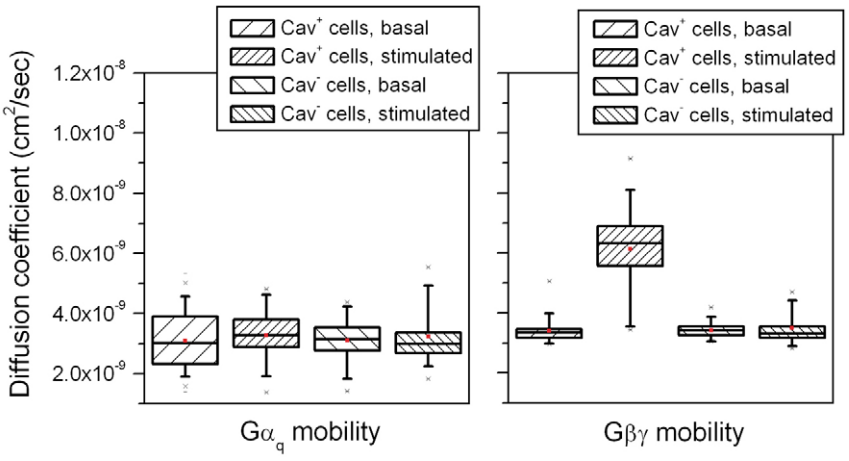

Fig. 3. Mobility of $G\alpha_q$ and $G\beta\gamma$ in FRTcav$^-$ and FRTcav$^+$ cells. Box-and-whisker diagram of the diffusion coefficient of $G\alpha_q$-eGFP (left) and eGFP-$G\beta\gamma$ (right) in FRTcav$^+$ and FRTcav$^-$ cells in the basal and stimulated (5 μM carbachol) state measured by FCS. The data set from each experiment is represented as a separate box. The boundary of the box is determined by the 25th and 75th percentiles, and the whiskers are determined by the 5th and 95th percentiles. The small red square within each box indicates the value of the mean for each set of data (n=20-50 per set; every D is calculated using a set of six to ten measurements of 10 seconds each). Data was collected with a band-pass emission filter (BP505-550) with excitation at 488 nm. For stimulated cells, data was recorded for 8 minutes post-stimulation from different cells and then averaged. All measurements were performed at ~25°C.

Mobility of $G\alpha_q$ and $G\beta\gamma$ in cells

We measured mobility of $G\alpha_q$-eGFP and eGFP-$G\beta\gamma$ in FRTcav$^-$ and FRTcav$^+$ cells, both in the basal and stimulated state, using FCS. FCS follows the temporal fluctuations of fluorescence intensity from a small number of fluorescent molecules moving in and out of a small open observation volume. Analysis of the temporal autocorrelation function, $G(\tau)$ calculated from this fluctuation data can yield the diffusion coefficient of the fluorescent molecule. We carried out multiple FCS measurements at room temperature on FRTcav$^+$ and FRTcav$^-$ cells transfected either with $G\alpha_q$-eGFP or with eGFP-$G\beta_1$ and HA-$G\gamma_7$ together. The autocorrelation function $G(\tau)$ obtained was best fitted to two diffusion coefficients: a fast diffusion (~2×10^{-7} cm^2/second), which is attributed to autofluorescence or movement of G proteins into the cytoplasm (see Discussion), and a slower one corresponding to the movement of G-protein subunits on the plasma membrane (Fig. 3). In unstimulated FRTcav$^-$ cells, the diffusion coefficient of $G\alpha_q$-eGFP was found to be $3.1\pm0.7\times10^{-9}$ cm^2/second (n=45) and the value remained unaltered upon stimulation ($3.2\pm0.9\times10^{-9}$ cm^2/second, n=34). Similar diffusion coefficients were measured for $G\alpha_q$-eGFP in FRTcav$^+$ cells (basal: $3.1\pm0.9\times10^{-9}$ cm^2/second, n=52; stimulated: $3.2\pm0.8\times10^{-9}$ cm^2/second, n=48) (Fig. 3A).

In contrast to the behavior seen for $G\alpha_q$-eGFP, the diffusion of eGFP-$G\beta_1$ and HA-$G\gamma_7$ expressed in FRTcav$^+$ cells increased from $3.4\pm0.5\times10^{-9}$ cm^2/second (n=19) to $6\pm1\times10^{-9}$ cm^2/second (n=19) upon stimulation (Fig. 3B). However, $G\beta\gamma$ diffusion remained unchanged in FRTcav$^-$ cells (basal: $3.4\pm0.3\times10^{-9}$ cm^2/second, n=14; stimulated: $3.5\pm0.5\times10^{-9}$ cm^2/second, n=17) (Fig. 3B). Overall, these data strongly suggest a significant change in association state for $G\beta\gamma$ in FRTcav$^+$ cells upon stimulation.

Cav1 expression induces sustained Ca^{2+} release in cells

If Cav1 is promoting the dissociation of $G\alpha_q$ and $G\beta\gamma$ subunits and/or inhibiting their recombination during cell stimulation, and if formation of the heterotrimeric G-protein complex is necessary for termination of the signal, we would expect that cells expressing Cav1 would stay stimulated for a longer period of time. We tested this idea by monitoring the downstream Ca^{2+} signal generated through PLCβ activation via carbachol stimulation of muscarinic receptors. As mentioned, PLCβ is activated by $G\alpha_q$ and/or $G\beta\gamma$ subunits coupled to muscarinic receptors. Activated PLCβ catalyzes the hydrolysis of phosphatidylinositol (4,5)-bisphosphate [PtdIns(4,5)P_2] to release Ins(1,4,5)P_3, which in turn increases the intracellular concentration of free Ca^{2+} (Rebecchi and Pentyala, 2000; Rhee, 2001). We monitored changes in Ca^{2+} in suspensions of FRTcav$^-$ and FRTcav$^+$ cells expressing PLCβ (both endogenous and transiently transfected) using FURA-2 AM, a cell-permeable fluorescent indicator for Ca^{2+} (Grynkiewicz et al., 1985).

In both FRTcav$^-$ and FRTcav$^+$ cells, stimulation of muscarinic receptors by 1 μM acetylcholine produces an identical transient Ca^{2+} spike that returned to basal levels after a few seconds (Fig. 4). The observation that both cell types show a similar amount of Ca^{2+} release with an identical timescale of release and recovery strongly suggests that the presence of Cav1 is not significantly altering the activity or concentration of components in this signaling pathway.

Because PLCβ is expressed at a much lower level as compared with $G\alpha_q$ (see Dowal et al., 2006a), it is possible that there is not enough of this enzyme to be affected by an increased amount of dissociated G-protein subunits. We thus transfected the cells with PLCβ1 or PLCβ2 to determine whether excess effector might allow us to better observe alterations in the duration of Ca^{2+} signaling. Both PLCβ1 and PLCβ2 are stimulated by $G\alpha_q$ subunits, whereas PLCβ2 can also be stimulated by $G\beta\gamma$ subunits (see Hepler et al., 1993; Smrcka and Sternweis, 1993). Comparison of the Ca^{2+} response generated by these two PLCβ variants in FRTcav$^-$ and FRTcav$^+$ cells would let us uncover possible differences in the level of activated $G\alpha_q$ and $G\beta\gamma$ subunits in two FRT cell types. Additionally, subjecting the cells to treatment with pertussis toxin only allows signaling through $G\beta\gamma$ subunits, helping to isolate the pathway involved in Ca^{2+} release.

We transfected FRTcav$^-$ and FRTcav$^+$ cells with similar levels of either PLCβ1 or PLCβ2, as determined by western blot analysis. FRTcav$^-$ cells transfected with either PLCβ variant yielded the same Ca^{2+} response as untransfected FRTcav$^-$ cells (Fig. 4). By contrast, a similar experiment with FRTcav$^+$ cells transfected with either PLCβ variant showed a significantly prolonged recovery time, suggesting sustained PLCβ stimulation (Fig. 4). The level of intracellular Ca^{2+} remained elevated for 2-3 minutes before returning to basal levels after 6-8 minutes. Interestingly, the peak time of sustained Ca^{2+} matched the timescale of the loss in FRET between $G\alpha_q$ and $G\beta\gamma$ (2 minutes and higher, Fig. 2B), suggesting that the longer time required for recombination of G-protein heterotrimers in FRTcav$^+$ cells is linked to the longer Ca^{2+} signal. Treating cells transfected with PLCβ2 with pertussis toxin reduced the amount of released Ca^{2+}, but did not affect the timescale of the sustained Ca^{2+} signal.

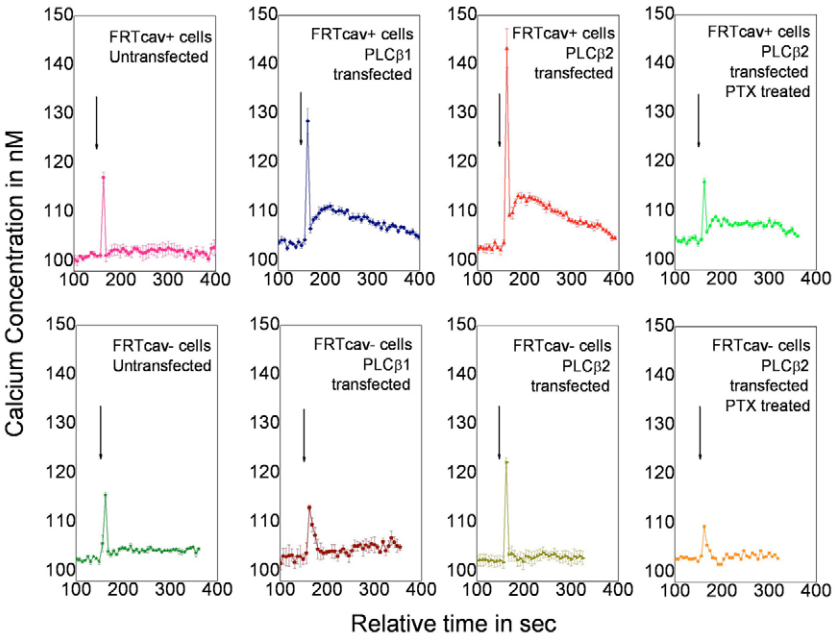

Fig. 4. The presence of Cav1 causes a sustained Ca^{2+} response. Change in intracellular Ca^{2+} in 1-ml suspensions of 10^6 FRTcav$^+$ or FRTcav$^-$ cells transfected with either empty vector, PLCβ1 or PLCβ2, and loaded with the Ca^{2+}-sensitive dye FURA-2AM upon addition of 1 μM acetylcholine (see Materials and Methods). *n*=6 of triplicate sets of samples. Black arrows indicate time of stimulus addition.

Activated $G\alpha_q$ preferentially binds to Cav1

We found that the presence of Cav1 promotes the dissociation of $G\alpha_q$-$G\beta\gamma$ and prolongs the Ca^{2+} recovery after stimulation in PLCβ-transfected cells. Several mechanisms can give rise to this behavior. First, in the presence of Cav1, $G\alpha_q$ and/or $G\beta\gamma$ might internalize in separate pathways upon stimulation, making their re-association less probable and therefore more time-consuming. Second, $G\alpha_q$ might move into Cav1 domains, leaving $G\beta\gamma$ upon stimulation, as has been previously suggested (Murthy and Makhlouf, 2000). Third, stimulation might enhance affinity between Cav1 and $G\alpha_q$ (localized in Cav1 domains), causing it to release $G\beta\gamma$ subunits. In this situation, the recombination of the heterotrimer would be delayed merely due to the tightly compacted nature of these domains that might hinder the diffusion of proteins.

To distinguish between the above mechanisms, we first determined whether the G-protein subunits internalize upon cell stimulation. Image analysis that monitored the amount of plasma membrane and cytosolic fluorescence from $G\alpha_q$-eYFP before and 10 minutes after stimulation showed that it remains bound to the plasma membrane after activation, in accord with previous studies using the same methodology (Dowal et al., 2006a; Philip et al., 2007). Similar results were obtained for eCFP-$G\beta\gamma$ (data not shown).

Next, we determined whether Cav1 and $G\alpha_q$ are colocalized in cells, and whether the extent of colocalization is altered upon stimulation. This study was done by transfecting FRTcav$^-$ cells with Cav1-eGFP and immunostaining the cells with a primary antibody against $G\alpha_q$ and a secondary antibody labeled with Alexa-Fluor-647. Cells were fixed before and 4 minutes after carbachol (5 μM) stimulation. The results (Fig. 5) show that the two proteins are colocalized in the basal state, giving a colocalization coefficient value of 0.35±0.05 (*n*=5). Stimulation with carbachol did not significantly change this value (0.43±0.11, *n*=7). The value for non-specific colocalization for these experiments was obtained using a control sample in which cells expressing Cav1-eGFP were immunostained without addition of the anti-$G\alpha_q$ primary antibody. The colocalization coefficient was 0.07 for this control. Although the spatial resolution achieved by immunofluorescence studies was low, these observations correlate well with co-immunoprecipitation studies showing that $G\alpha_q$ and Cav1 interact (Oh and Schnitzer, 2001), and support the idea that $G\alpha_q$ might reside in caveolae domains before and after cell stimulation.

To determine whether $G\alpha_q$ binds directly to Cav1 (Murthy and Makhlouf, 2000), we first compared the binding of purified G proteins to membranes prepared from FRTcav$^-$ or FRTcav$^+$ cells. These studies were done by covalently labeling $G\alpha_q$(GDP),

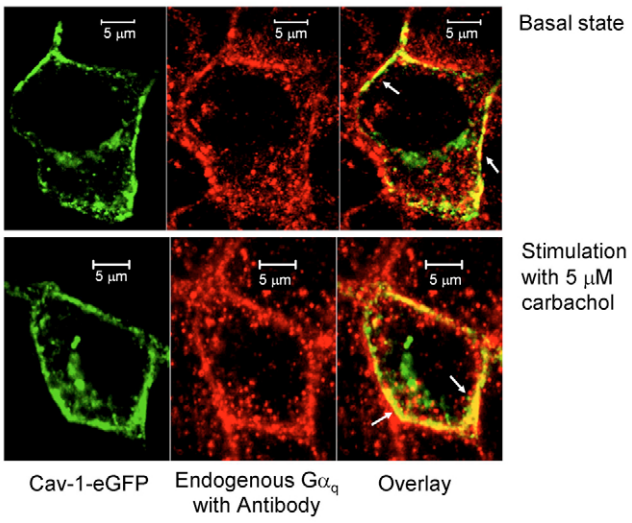

Fig. 5. Immunofluorescence confocal images showing the colocalization of Cav1 and $G\alpha_q$. Confocal images of fixed FRT cells expressing transiently transfected Cav1-eGFP (green) are immunostained for endogenous $G\alpha_q$ (red). Yellow pixels in the merged images indicate colocalization. Cells were either fixed without stimulation (top) or at 4 minutes after stimulation with 5 μm carbachol (bottom). Images were recorded with emission filter sets BP505-530 (green) and LP650 (red) using two separate lasers for sequential excitation (488 nm for green and 633 nm for red).

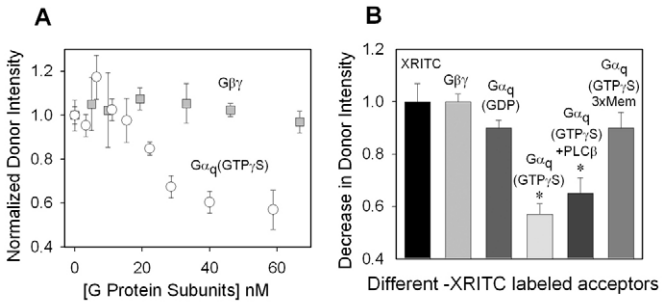

Fig. 6. FRET illustrates that activated $G\alpha_q$ has a stronger affinity for Cav1-eGFP than do $G\beta\gamma$ subunits. (A) The titration curve of XRITC-$G\beta\gamma$ and XRITC-$G\alpha_q$(GTPγS), showing the normalized decrease in Cav1-eGFP intensity as the G proteins are added, caused by energy transfer (FRET). (B) Bar graph showing the values of the normalized donor intensities for free acceptor XRITC at 60 nM (n=2), XRITC-$G\beta\gamma$ at 70 nM (n=3), XRITC-$G\alpha_q$(GDP) (n=3), XRITC-$G\alpha_q$(GTPγS) (n=5), XRITC-$G\alpha_q$(GTPγS) + 80 nM PLCβ1 (n=2) and XRITC-$G\alpha_q$ (GTPγS) starting with threefold the initial amount of Cav1-eGFP-containing FRTcav$^-$ membranes (n=3). Asterisks indicate significant difference, P<0.001, by one-way variance from control.

$G\alpha_q$(GTPγS) and $G\beta\gamma$ with the fluorescent probe CPM and monitoring the increase in fluorescence as the proteins bind to the FRTcav$^-$ or FRTcav$^+$ cell membranes (see Philip and Scarlata, 2006). Binding studies, performed in triplicate, of 5 nM CPM-$G\beta\gamma$ to the two sets of membrane yielded binding constants that averaged 8.7±1.3 nM (n=4 for each set of three) with no statistical significance between the two groups. By contrast, the binding constants calculated for CPM-$G\alpha_q$(GDP) with FRTcav$^-$ or FRTcav$^+$ cell membranes were 3.2±0.5 nM (n=12) and 1.3±0.2 nM (n=8), respectively. These data indicate that CPM-$G\alpha_q$(GDP) binds ~threefold more strongly to Cav1-containing membranes.

In a second series of membrane-binding studies, we monitored the association between purified G-protein subunits labeled with a FRET acceptor (XRITC) and Cav1-eGFP, in which the eGFP tag on Cav1 acts as a FRET donor (see Philip et al., 2007). These studies were carried out by preparing membranes from FRTcav$^-$ cells expressing Cav1-eGFP and monitoring the loss in eGFP fluorescence as the protein with labeled acceptor was incrementally added (see Materials and Methods). Fig. 6A shows the full titration curves for XRITC-$G\beta\gamma$ and XRITC-$G\alpha_q$(GTPγS), and Fig. 6B shows the corresponding summary of different samples at the endpoint of the titration. No loss in donor fluorescence was observed when the free fluorophore, XRITC, or labeled $G\beta\gamma$ subunits were added, indicating a lack of interaction between Cav1-eGFP and these species. Alternately, a small decrease was seen when labeled $G\alpha_q$(GDP) was used. Importantly, a large and significant decrease was observed when labeled $G\alpha_q$(GTPγS) was added, suggesting a specific interaction between activated $G\alpha_q$ and Cav1. A similar decrease was noted for activated $G\alpha_q$ with 80 nM PLCβ2, showing that the presence of effector does not disrupt $G\alpha_q$(GDP)–Cav1-eGFP interactions.

To support the idea that the decrease in Cav1-eGFP donor intensity upon the addition of XRITC-$G\alpha_q$(GTPγS) represents a true protein-protein association, the titration was repeated using a threefold higher concentration of Cav1-eGFP-containing membranes. This higher concentration would be expected to shift the titration curve to higher $G\alpha_q$(GTPγS) concentrations and reduce the amount of FRET at 60 nM of added acceptor. As shown in Fig. 6, the amount of FRET, as seen by a decrease in donor intensity, was reduced when the concentration of membranes was raised. Taken together, these studies suggest that activated $G\alpha_q$(GTPγS), but not $G\beta\gamma$, specifically interact with Cav1-eGFP.

Discussion

Cav1 has been shown to organize into plasma membrane domains called caveolae, which are involved in localizing signaling proteins (Liu et al., 2002; Pelkmans and Helenious, 2002). However, it is still unclear why some cell lines contain caveolae whereas others do not. The studies presented here surprisingly show that the domains formed by Cav1 have the ability to alter the duration of Ca^{2+} signaling mediated through the G-protein subunits $G\alpha_q$ and $G\beta\gamma$.

Our studies used a cell line that does not contain caveolae because of lack of Cav1 expression and a sister line stably transfected with Cav1 that forms domains similar in size and structure to caveolae. These cell lines have been used as a model for other caveolae studies (Lipardi et al., 1998; Mora et al., 1999). We verified the plasma membrane localization of Cav1 and the G-protein subunits in attached cells by imaging Cav1-eGFP, and in cell suspensions by cell fractionation and western blot analysis. We found that the fluorescent-tagged G-protein subunits were similarly expressed and plasma-membrane localized in both cell lines. Importantly, we also found that the extent and timing of Ca^{2+} release and recovery were the same in both cell lines, suggesting that the expression of Cav1 does not significantly affect the level of expression or activity of proteins involved in Ca^{2+} release. It is also noteworthy that the fluorescent-tagged G-protein subunits were overexpressed by a low amount and were not expected to affect the complexation (see Dowal et al., 2006a; Philip et al., 2007), although overexpression would stabilize G-protein heterotrimers, which was not observed here for the FRTcav$^+$ cells.

The Ca^{2+} measurements were performed on suspension cells, whereas the microscopy studies imaged attached cells. It has been observed that detachment of cells from the extracellular matrix can cause time-dependent movement of Cav1 from the plasma membrane to the cytosol (e.g. del Pozo et al., 2005; Pelkmans et al., 2002) and it is possible that a portion of Cav1 might have internalized in the studies involving cells in suspension. However, this movement of Cav1 from the membrane to the internal compartment of the cells would diminish the sustained Ca^{2+} release observed for FRTcav$^+$ cells, potentially making the true effect of Cav1 on Ca^{2+} responses more pronounced.

We focused on activation of muscarinic receptors, which internalize through a clathrin-mediated pathway (Tobin, 1997), although it is possible that these receptors also use a caveolae-mediated pathway when available (Dessy et al., 2000). We note that the observed Ca^{2+} desensitization rates were similar in the presence and absence of Cav1, and thus, if Cav1 was involved in receptor sequestration and recycling, this process must occur at the same rate as their clathrin counterparts.

There is increasing evidence that heterotrimeric G proteins are pre-coupled to receptors in the basal state of cells (Nobles et al., 2005) and thus the localization of receptors would in turn determine the localization of their attached G proteins. However, the sequestration of different GPCRs in caveolae domains might be cell-type specific (see Ostrom 2002; Ostrom et al., 2001) and so it is difficult to predict their localization in these studies. Although it is possible that the receptors and associated $G\alpha_q$ subunits are outside Cav1 domains in the basal state and relocalize to these domains upon cell stimulation, as suggested in previous immunoblotting

studies (Murthy and Makhlouf, 2000), our co-immunofluorescence data instead suggest that $G\alpha_q$ proteins are localized in or close to Cav1 in the basal state and do not undergo detectable change in colocalization upon cell stimulation.

A direct comparison of basal-state FRET values of eCFP-$G\beta\gamma$ and $G\alpha_q$-eYFP in FRTcav$^-$ and FRTcav$^+$ cells show that they are identical, suggesting that the presence of Cav1 does not influence their association via preferential partitioning. Based on the size of the eCFP- and eYFP-tagged proteins and the distance at which 50% FRET occurs for these probes [45-49 Å (Patterson et al., 2000)], the two G-protein subunits must be in contact in order to transfer energy (for details, see Dowal et al., 2006a). In both cell types, the level of FRET from eCFP-$G\beta\gamma$ to $G\alpha_q$-eYFP increased upon stimulation. This increase in FRET upon stimulation has been previously reported for eCFP-$G\beta\gamma$ and $G\alpha_i$-eYFP with similarly placed eCFP and eYFP tags (Bunemann et al., 2003), and is thought to be caused by reorientation of the tags on the G-protein subunits upon stimulation that allow for more-efficient transfer of energy.

FRET studies showed that, in FRTcav$^-$ cells, the initial high FRET value between eCFP-$G\beta\gamma$ and $G\alpha_q$-eYFP returned to its basal level after ~1 minute. Surprisingly, in FRTcav$^+$ cells, the normalized FRET from eCFP-$G\beta\gamma$ to $G\alpha_q$-eYFP continued to decrease with time to a level close to or below our detection limit. The simplest explanation is that Cav1 is promoting a physical separation of $G\alpha_q$ from $G\beta\gamma$ subunits after stimulation in FRTcav$^+$ cells.

To authenticate the separation of G-protein subunits in FRTcav$^+$ cells upon stimulation, we used FCS to determine the mobility of G-protein subunits in basal and stimulated FRTcav$^+$ and FRTcav$^-$ cells. The diffusion coefficients of $G\alpha_q$ and $G\beta\gamma$ are close to each other in the basal state of both cell types, and closely match the diffusion of receptors in membranes (e.g. Barak et al., 1997; Hegener et al., 2004; Kenworthy et al., 2004). Because we have found that $G\alpha_q$ and $G\beta\gamma$ can associate with GPCRs in resting cells (Philip et al., 2007), then it is highly probably that the G proteins reside in a complex with receptor. Lipidated G-protein subunits would diffuse faster on membrane if not attached to the receptors (Kenworthy et al., 2004).

The diffusion of $G\alpha_q$ does not change upon stimulation, suggesting a stable association. A lack of change in mobility for $G\beta\gamma$ upon stimulation is also seen in FRTcav$^-$ cells expressing eGFP-$G\beta_1$ and $G\gamma_7$. These results support the idea that certain G-protein families reside in stable signaling complexes through the activation cycle to activate effectors (e.g. Bunemann et al., 2003; Evanko et al., 2005; Philip et al., 2007). However, in FRTcav$^+$ cells, the diffusion coefficient of $G\beta\gamma$ increases twofold upon stimulation. This faster movement of $G\beta\gamma$ in the presence of Cav1, in addition to its loss of FRET with $G\alpha_q$, suggests that, upon stimulation, it detaches from its local signaling complex. This increased mobility is only seen for $G\beta\gamma$ subunits in FRTcav$^+$ cells upon stimulation and is similar to other lipidated membrane-associated proteins (Kenworthy et al., 2004). This strongly indicates physical dissociation of $G\beta\gamma$ subunits from $G\alpha_q$–receptor complexes. FCS measurements also show that $G\beta\gamma$ remains free even at 8 minutes post-stimulation. We note that certain families of G-protein subunits have been found to physically dissociate after receptor activation (e.g. Digby et al., 2006; Frank et al., 2005; Hein et al., 2006; Janetopoulos et al., 2001).

A fast component, which is indicative of diffusion of a small molecule or protein in the cytoplasm, is present at a contribution of ~50% in all of the FCS measurements in cells expressing either $G\alpha_q$-eGFP or eGFP-$G\beta_1$ and $G\gamma_7$. We argued that this component corresponds to autofluorescence (see Philip et al., 2007). For our $G\beta\gamma$-diffusion measurements, this fast component might also arise from cytosolic eGFP-$G\beta_1$, because membrane binding of $G\beta1$ is promoted by $G\gamma$ subunits and it is possible that the local concentration of $G\gamma$ was not sufficient to drive complete membrane association. The problem of a cytosolic component is compounded by the thinness of the membrane, which covers a vanishing axial fraction of the observation volume for FCS measurements. Thus, fluorescent molecules in the cytoplasm will always contribute to the reading. However, the diffusion of this component was 15- to 40-times faster and did not interfere with the detection of the slower membrane-bound component. Also, the increase in the diffusion of the membrane-bound eGFP-$G\beta\gamma$ with stimulation in FRTcav$^+$ cells was significant, whereas the diffusion of the faster component remained unaltered.

We determined whether Cav1 influences the membrane-binding affinity of the G-protein subunits $G\alpha_q$ and $G\beta\gamma$. We found that, even though $G\beta\gamma$ binds similarly to membranes prepared from FRTcav$^-$ and FRTcav$^+$ cells, $G\alpha_q$ binds more strongly to membranes prepared from cells expressing Cav1. This observation fits well into previous experiments showing that $G\alpha_q$, but not $G\beta\gamma$ or $G\alpha_i$, localize to caveolae fractions (Oh and Schnitzer, 2001). The interaction between Cav1 and $G\alpha_q$ in cells has been demonstrated by cell-fractionation studies using glutathione S-transferase (GST) and co-immunoprecipitation techniques (deWeerd and Leeb-Lundberg, 1997; Li et al., 1995; Liu et al., 2002; Lockwich et al., 2000; Smart et al., 1995). Our colocalization and in vitro FRET data between Cav1-eGFP and XRITC-labeled G proteins illustrate that $G\alpha_q$ is strongly associated with caveolae domains even after stimulation, agreeing with similar experiments in the literature (Murthy and Makhlouf, 2000). We found that activated $G\alpha_q$, but not $G\beta\gamma$, subunits preferentially bind to Cav1. Keeping in mind that the affinity between $G\alpha_q$ and $G\beta\gamma$ is substantially weakened upon activation (Runnels and Scarlata, 1999), we suggest that, in the activated state, $G\alpha_q$ interacts preferentially with Cav1. This relative enhancement of $G\alpha_q$-Cav1 interactions over $G\alpha_q$-$G\beta\gamma$ might cause release of $G\beta\gamma$ from $G\alpha_q$, resulting in physical separation of the heterotrimer. This physical separation allows for faster mobility of $G\beta\gamma$ and causes its recombination with $G\alpha_q$ subunits to be diffusion-limited. In addition, Cav1 crowds the membrane, imposing diffusion barriers (Schlegel et al., 1998). Because we monitored FRET, which depends on the sixth power of the distance, the separation between the G-protein subunits need not be far. However, the altered membrane composition might delay the diffusion-limited reformation of the heterotrimer, prolonging the elevated Ca^{2+} signal.

Importantly, we found that the separation between $G\alpha_q$ and $G\beta\gamma$ caused by Cav1 expression can affect the temporal aspects of the cell signal. Ca^{2+} recovery was prolonged in PLCβ-transfected cells only when Cav1 was present. This increased duration was over several minutes. Also, we only observed prolonged high Ca^{2+} levels in the presence of excess effector that has GAP activity, suggesting that the Ca^{2+} response is limited at the level of effector in these cells. We found that the Ca^{2+} spike occurs in the first 40 seconds, coincident with the FRET increase (Fig. 4). After, the slower, sustained signal becomes prominent, correlating with the loss in FRET (>110 seconds), suggesting a correlation between the times of the two types of FRET changes and the two types of Ca^{2+} responses. Our results correlate well with studies showing that activation of M_3 receptors causes PLC-mediated PtdIns(4,5)P_2

hydrolysis, generating Ins(1,4,5)P_3, which mobilizes intracellular Ca^{2+} (Ding et al., 1997).

Our data indicate that the sustained Ca^{2+} signal is due to the Cav1-Gα_q-PLCβ complex, as well as PLCβ2, interacting with released Gβγ. The in vitro FRET binding studies show that the presence of PLCβ1 far above the equilibrium constant for dissociation (K_d) does not affect Gα_q-Cav1 binding, supporting this idea (Fig. 6B) and suggesting that the interaction sites for Cav1 and PLCβ on Gα_q are distinct. We found that transfection of PLCβ2 results in a higher level of Ca^{2+} release as compared with PLCβ1 transfection (Fig. 4). Also, we observed a reduced but extended Ca^{2+} signal in FRTcav$^+$ cells transfected with PLCβ2 and pre-treated with pertussis toxin, which only allows signaling through Gβγ subunits (Fig. 4). This suggests a contribution of Gβγ-PLCβ2 to the sustained Ca^{2+} signal.

Dissociation of G-protein subunits can impact signaling profoundly by allowing the dissociated subunits to interact with alternate effectors. This can be important for signaling diversity and receptor cross-talk through Gβγ exchange (Quitterer and Lohse, 1999). Gβγ subunits are regulators of certain Ca^{2+} channels and modulation of Ca^{2+} can occur via activation of PKC through activated Gα_q (Dascal, 2001; Strock and Diversé-Pierluissi, 2004; Wickman and Clapham, 1995). Here, the observed physical separation of Gα_q and Gβγ, and Ca^{2+} mobilization, are very specific to Cav1 expression, and the control cells (FRTcav$^-$) showed no such effect under identical experimental conditions. It is possible that downstream effectors (PLCβ and/or PKC) and Ca^{2+}-release-activated Ca^{2+} (CRAC) channels also require Cav1 to function. However, our data illustrate that the initial events in the signaling pathway involving M_3-receptor–Gα_q–Gβγ–PLCβ are distinct when Cav1 is present. Presence of free Gβγ subunits, at 8 minutes post-stimulation in FRTcav$^+$ cells, can drastically alter a range of signaling pathways. Our results also correlate well with previous speculation that caveolae domains are involved in Ca^{2+} signaling involving Gα_q (Balijepalli et al., 2005; Isshiki and Anderson, 1999; Kamishima et al., 2007). Although the effects of this potential sequestration of Gα_q by Cav1 on Ca^{2+} signals in more natural systems are unclear, these studies offer the possibility of using Cav1 as a tool to modify Ca^{2+} responses. It is interesting to speculate the role of Cav1 in modulating the time-scale of other signaling events.

Materials and Methods

Materials

G-protein constructs eGFP-Gβ_1, eCFP-Gβ_1, HA-Gγ_7, Gα_q-eGFP and Gα_q-eYFP were provided by Catherine Berlot (Geisinger Clinic, Danville, PA) (Hughes et al., 2001). FRTcav$^-$ cells, which do not express Cav1, and FRTcav$^+$ cells stably transfected with canine Cav1 or canine eGFP-Cav1 construct were gifts from Deborah Brown (Stony Brook University, NY). G-protein subunits were expressed in Sf9 cells and purified as previously described (Runnels and Scarlata, 1999).

Cell culture and transfection of FRT cells

FRTcav$^-$ and FRTcav$^+$ cells were maintained in F-12 Coon's modified media containing 10% FBS (Gemini Bioproducts). Medium of FRTcav$^+$ cells was supplemented with 200 μg/ml G-418 (Sigma) to preferentially select cells expressing Cav1. Cells maintained in 60-mm dishes were transfected by mixing DNA with lipofectamine reagent (Lipofectamine 2000, Invitrogen) following the manufacturer's protocol. The medium of the cells was replaced with fresh medium after 6-8 hours of incubation with the lipofectamine-DNA mixture. For imaging, FRET and FCS experiments, transfected cells were grown in glass bottom dishes (MatTek).

Isolation of total membrane fraction

Harvested cells were washed twice with PBS and centrifuged at 5000 ***g*** for 5 minutes. Aprotinin and protease inhibitor cocktail were added to the pellet obtained. The cells were homogenized and centrifuged at 5000 ***g*** for 5 minutes at 4°C. Resulting supernatant was spun at 50,000 ***g*** for 35 minutes at 4°C to collect the pellet, which corresponds to total membrane fraction. The concentration of total membrane protein was measured with protein assay and the phospholipid concentration was assessed by phosphate analysis.

Fluorescence-based membrane-binding studies

Gα_q and Gβγ subunits were labeled with CPM [7-diethylamino-3-(4′-maleimidylphenyl)-4-methylcoumarin] (Philip and Scarlata, 2004; Philip et al., 2007). Natural membrane fractions from FRTcav$^-$ or FRTcav$^+$ cells were added to 120 μl 50 nM CPM-Gα_q or CPM-Gβγ subunits in a 3-mm square cuvette, and the integrated intensity was monitored by exciting the sample at 384 nm and scanning the fluorescence from 420 to 540 nm. After correcting for background from control samples and dilution, the normalized changes in emission energies were plotted and fit to obtain an apparent partition coefficient, K_p. Here, membrane concentrations are expressed in terms of the total protein content, as measured by Bradford analysis and total phosphate levels, determined by the malachite green method (Itaya and Ui, 1966).

FRET between eGFP and XRITC

G proteins were labeled with the rhodamine probe XRITC (X-rhodamine isothiocyanate, Invitrogen) (Philip and Scarlata, 2004; Philip et al., 2007). XRITC-Gα_q was activated using GTPγS (Chiadac et al., 1999), in which GDP was substituted as a control. Membranes from FRTcav$^-$ cells transiently transfected with Cav1-eGFP were diluted 12-fold with buffer (150 mM NaCl, 20 mM HEPES, pH 7.2, and 20 mM βME) so that the eGFP fluorescence intensity at 523 nm was similar to 60 nM XRITC signal at 600 nm also exciting at 480 nm.

FRET measurements were carried out by exciting the sample at 480 nm and recording the fluorescence intensities at 523 nm (donor) and 600 nm (acceptor). The loss in donor fluorescence gave less error than the increase in acceptor fluorescence and so only the donor intensities were used for final calculation. Control samples that substituted buffer for XRITC probes showed no change in 523-nm intensity when corrected for dilution. Donor intensities were corrected for acceptor contribution by subtracting the intensities from XRITC samples titrated into buffer only.

Measurement of cellular Ca^{2+}

Ca^{2+} levels were determined using Fura-2-AM (Invitrogen) in an ISS PC1 spectrofluorometer, as previously described (Dowal et al., 2006b; Guo et al., 2005): cells were suspended, labeled with 1 μM Fura-2-AM, and the ratio of fluorescence intensities at 510 nm was monitored by exciting the sample at 340 and 380 nm. The intensity ratios were monitored for 10 minutes, during which the cells were stimulated with 1 μM acetylcholine and lysed with 10% Triton X, followed by addition of 400 nM EDTA. Each event was separated by 2-3 minutes. The intensity ratio was converted into Ca^{2+} concentration as before.

Immunofluorescence staining

FRTcav$^-$ cells expressing Cav1-eGFP were grown in glass bottom imaging dishes and were washed twice with PBS, followed by the addition of 3% paraformaldehyde for 20 minutes. If required, cells were stimulated using carbachol before fixation. Cells were washed three times for 10 minutes with 0.5% Triton X-100 in PBS, and blocked in PBS containing 5% goat serum, 1% BSA and 50 mM glycine for 45 minutes. Next, anti-Gα_q primary antibody (from rabbit, Santa Cruz) with 1:200 dilution in PBS + 1% BSA was added followed by incubation at 37°C for 45 minutes. Cells were then washed three times for 10 minutes with PBS + 1% BSA, followed by addition of Alexa-Fluor-647-labeled anti-rabbit secondary antibody (Invitrogen) diluted to 1:1000 in PBS + 1% BSA and subsequent incubation at 37°C for 45 minutes. After washing the cells three times with PBS, they were viewed in PBS in LSM510-Meta (Carl Zeiss, Jena, Germany).

Fluorescence imaging for FRET experiments in cells

Images of cells overexpressing fluorescent-tagged Gβγ and/or Gα_q were taken on an Zeiss Axiovert 200M microscope as previously described (Dowal et al., 2006a). Energy transfer between Gα_q-eYFP and eCFP-Gβγ pairs was measured by taking images of cells co-expressing the eCFP- and eYFP-tagged proteins under three sets of filter cubes from Chroma, CFP, YFP and FRET (CFP: 31044v2; exciter D436/20x, dichroic 460DCLP, emitter D480/40m; YFP: 41029; exciter HQ500/20x, dichroic Q515LP, emitter HQ520LP and FRET: 31052; exciter D436/20x, dichroic 460DCLP, emitter D535/30m). The resulting image intensity from each channel was corrected for photobleaching by dividing the image intensity by e^{-kt}, in which k is the rate of decay. Rate of decay for each filter was obtained by fitting intensity values from photobleached cells expressing either CFP or YFP. Under our experimental conditions, eYFP did not show any photobleaching. Afterwards, a normalized FRET (N_{FRET}) value was calculated (Xia and Liu, 2001): $N_{FRET} = [I_{FRET} - (I_{CFP} \times \alpha) - (I_{YFP} \times \beta)] / [(I_{CFP} \times I_{YFP})^{1/2}]$, in which α and β are CFP and YFP bleed-through emissions in the FRET channel, respectively. A plug-in, created in ImageJ, was used to obtain images showing pixel intensities that correspond to normalized FRET values.

Confocal imaging and colocalization experiments

Cells were imaged on an Axiovert 200M microscope equipped with multi-line laser excitation and a 40×/1.2 NA apochromat water immersion objective. Cav1-eGFP was imaged using 488-nm Ar-ion laser line in ConfoCor2 (Carl Zeiss, Jena, Germany) using a BP505-530 emission filter. Endogenous Gα_q immunolabeled with

Alexa-Fluor-647 was imaged using a 633-nm line from a He:Ne laser and with LP650 emission filter. The two fluorophores were excited in a sequential manner using Multi Track acquisition. This procedure eliminates channel cross-talk completely. Data analysis for colocalization was performed using AIM software provided with Zeiss LSM510-Meta.

Fluorescence-correlation-spectroscopy measurements

FCS measurements were performed with an Axiovert 200M microscope with a ConfoCor2 unit equipped with a 40×/1.2 NA water immersion objective (Apochromat) and a continuous argon ion laser (Carl Zeiss, Jena, Germany). Excitation of the fluorophore (eGFP) was at 488 nm with an incident laser power of 20 μW, and the fluorescence was recorded using an avalanche photodiode through a band-pass emission filter (BP505-550). The time trace of the fluorescence was analyzed by a digital temporal correlator to compute the autocorrelation function, $G(\tau)$. The observation volume for FCS experiment was determined by calibrating the instrument with a 2 nM aqueous solution of Alexa-Fluor-488 of known diffusion coefficient ($D_{\text{Alexa488}} = 2.2\times10^{-6}$ cm^2/second). All measurements were done at room temperature (~25°C). Autocorrelation functions, $G(\tau)$s, were analyzed using the fitting routine for two-dimensional diffusion provided by Zeiss with ConfoCor2 software. We use the following equation: $G(\tau)=\Sigma a_i\,(1+\tau/\tau_D)^{-1}$, in which τ_D is the residence time of a molecule in FCS observation volume and a_i is the relative contribution of the ith species in the autocorrelation. The diffusion coefficient, D, is calculated from τ_D of a molecule using Einstein relation for diffusion: $r^2=4D.\tau_D$, in which r is the radius of the observation volume (for details, see Maiti et al., 1997; Sengupta et al., 2002).

The authors are grateful to Deborah Brown, Louisa Dowal and Catherine Berlot for sharing their reagents, and thank Paxton Provitera for his help with FRET analysis, Stuart McLaughlin for the use of his Conforcor2 instrument, and Mario Rebecchi and Deborah Brown for their helpful suggestions. This work was supported by NIH GM053132.

References

Anderson, R. G. (1998). The caveolae membrane system. *Annu. Rev. Biochem.* **67**, 199-225.

Balijepalli, R. C., Foell, J. D., Hall, D. D., Hell, J. W. and Kamp, Y. J. (2005). Localization of cardiac L-type Ca2+ channels to a caveolar macromolecular signaling complex is required for beta2-adrenergic regulation. *Proc. Natl. Acad. Sci. USA* **103**, 7500-7505.

Barak, L. S., Ferguson, S. S., Zhang, J., Martenson, C., Meyer, T. and Caron, M. G. (1997). Internal trafficking and surface mobility of a functionally intact beta2-adrenergic receptor-green fluorescent protein conjugate. *Mol. Pharmacol.* **51**, 177-184.

Bunemann, M., Frank, M. and Lohse, M. J. (2003). Gi protein activation in intact cells involves subunit rearrangement rather than dissociation. *Proc. Natl. Acad. Sci. USA* **100**, 16077-16082.

Chiadac, P., Mavkin, V. S. and Ross, E. M. (1999). Kinetic control of guanine nucleotide binding to soluble Gαq. *Biochem. Pharmacol.* **58**, 39-48.

Dascal, N. (2001). Ion-channel regulation by G proteins. *Trends Endocrinol. Metab.* **12**, 391-398.

del Pozo, M. A., Balasubramanian, N., Alderson, N. B., Kiosses, W. B., Grande-Garcia, A., Anderson R. G. W. and Schwartz, M. A. (2005). Phospho-caveolin-1 mediates integrin-regulated membrane domain internalization. *Nat. Cell Biol.* **7**, 901-908.

Dessy, C., Kelly, R. A., Balligand, J. L. and Feron, O. (2000). Dynamin mediates caveolar sequestration of muscarinic cholinergic receptors and alteration in NO signaling. *EMBO J.* **19**, 4272-4280.

deWeerd, W. F. and Leeb-Lundberg, L. M. (1997). Bradykinin sequesters B2 bradykinin receptors and the receptor-coupled Gα subunits Gαq and Gαi in caveolae in DDT MF-2 smooth muscle cells. *J. Biol. Chem.* **272**, 17858-17866.

Digby, G. J., Lober, R. M., Sethi, P. R. and Lambert, N. A. (2006). Some G protein heterotrimers physically dissociate in living cells. *Proc. Natl. Acad. Sci. USA* **103**, 17789-17794.

Ding, K.-H., Husain, S., Akhtar, R. A., Isales, C. M. and Abdel-Latif, A. A. (1997). Inhibition of muscarinic-stimulated polyphosphoinositide hydrolysis and Ca+2 mobilization in cat iris sphincter smooth muscle cells by cAMP-elevating agents. *Cell. Signal.* **9**, 411-419.

Dowal, L., Provitera, P. and Scarlata, S. (2006a). Gαq and its effector Phospholipase Cβ1 are complexed in the basal state. *J. Biol. Chem.* **281**, 23999-24014.

Dowal, L., Provitera, P. and Scarlata, S. (2006b). Stable association between G alpha(q) and phospholipase C beta 1 in living cells. *J. Biol. Chem.* **281**, 23999-24014.

Evanko, D. S., Thiyagarajan, M. M., Takida, S. and Wedegaertner, P. B. (2005). Loss of association between activated G[alpha]q and G[beta][gamma] disrupts receptor-dependent and receptor-independent signaling. *Cell. Signal.* **17**, 1218-1228.

Frank, M., Thumer, L., Lohse, M. J. and Bunemann, M. (2005). G-protein-activation without subunit dissociation depends on a Galpha i-specific region. *J. Biol. Chem.* **280**, 24584-24590.

Grynkiewicz, G., Poenie, M. and Tsien, R. Y. (1985). A new generation of Ca^{2+} indicators with greatly improved fluorescence properties. *J. Biol. Chem.* **260**, 3440-3450.

Guo, Y., Rebecchi, M. and Scarlata, S. (2005). Phospholipase $C\beta_2$ binds to and inhibits phospholipase $C\delta_1$. *J. Biol. Chem.* **280**, 1438-1447.

Hegener, O., Prenner, L., Runkel, F., Baader, S. L., Kappler, J. and Haberlein, H. (2004). Dynamics of β2-adrenergic receptor-ligand complexes on living cells. *Biochemistry* **43**, 6190-6199.

Hein, P., Rochais, F., Hoffmann, C., Dorsch, S., Nikolaev, V. O., Engelhardt, S., Berlot, C. H., Lohse, M. and Buneman, M. (2006). G_s activation is time-limiting in initiating receptor-mediated signaling. *J. Biol. Chem.* **281**, 33345-33351.

Hepler, J. R., Kozasa, T., Smrcka, A. V., Simon, M. I., Rhee, S. G., Sternweis, P. C. and Gilman, A. G. (1993). Purification from Sf9 cells and characterization of recombinant Gq alpha and G11 alpha. Activation of purified phospholipase C isozymes by G alpha subunits. *J. Biol. Chem.* **268**, 14367-14375.

Hughes, T. E., Zhang, H. and Logothetis de Berlot, C. H. (2001). Visualization of a functional Galpha q-green fluorescent protein fusion in living cells. Association with the plasma membrane is disrupted by mutational activation and by elimination of palmitoylation sites, but not be activation mediated by receptors or AlF4. *J. Biol. Chem.* **276**, 4227-4235.

Isshiki, M. and Anderson, R. G. W. (1999). Calcium signal transduction from caveolae. *Cell Calcium* **26**, 201-206.

Itaya, K. and Ui, M. (1966). A new micromethod for the colorimetric determination of inorganic phosphate. *Clin. Chim. Acta* **14**, 361-366.

Janetopoulos, C., Jin, T. and Devreotes, P. (2001). Receptor -mediated activation of heterotrimeric G-proteins in living cells. *Science* **291**, 2408-2411.

Jimenez, E., Pavia, J., Morell, V., Martin, E. and Montiel, M. (2001). Muscarinic receptor subtypes and calcium signaling in Fischer rat thyroid cells. *Biochem. Pharmacol.* **61**, 337-342.

Kamishima, T., Burdyga, T., Gallagher, J. A. and Quayle, J. M. (2007). Caveolin-1 and caveolin-3 regulate Ca2+ homeostasis of single smooth muscle cells from rat cerebral resistance arteries. *Am. J. Physiol. Heart Circ. Physiol.* **293**, H204-H214.

Kenworthy, A. K., Nichols, B. J., Remmert, C. L., Hendrix, G. M., Kumar, M., Zimmerberg, J. and Lippincott-Schwartz, J. (2004). Dynamics of putative raft-associated proteins at the cell surface. *J. Cell Biol.* **165**, 735-746.

Kim, C.-H., Park, Y.-S., Chung, K.-N. and Elwood, P. C. (2002). Sorting and function of the human folate receptor is independent of the cavolein expression in Fisher rat thyriod epithelial cells. *Biochem. Mol. Biol.* **35**, 395-402.

Lakowicz, J. (1999). *Principles of Fluorescence Spectroscopy* (2nd edn). New York: Plenum.

Li, S., Okamoto, T., Chun, M., Sargiacomo, M., Cassanova, J. E., Hansen, S. H., Nishimoto, I. and Lisanti, M. P. (1995). Evidence for a regulated interaction between heterotrimeric G proteins and caveolin. *J. Biol. Chem.* **270**, 15693-15701.

Lipardi, C., Mora, R., Colomer, V., Paladino, S., Nitsch, L., Rodriguez-Boulan, E. and Zurzolo, C. (1998). Caveolin transfection results in caveolae formation but not apical sorting of glycosylphosphatidylinositol (GPI)-anchored proteins in epithelial cells. *J. Cell Biol.* **140**, 617-626.

Liu, P., Rudick, M. and Anderson, R. G. W. (2002). Multiple functions of caveolin-1. *J. Biol. Chem.* **277**, 41295-41298.

Lockwich, T. P., Liu, X., Singh, B. B., Jadlowiec, J., Weiland, S. and Ambudkar, I. S. (2000). Assembly of Trp1 in a signaling complex associated with caveolin-caffolding lipid raft domains. *J. Biol. Chem.* **275**, 11934-11942.

Maiti, S., Haupts, U. and Webb, W. W. (1997). Fluorescence correlation spectroscopy: diagnostics for sparse molecules. *Proc. Natl. Acad. Sci. USA* **94**, 11753-11757.

Marx, J. (2001). Caveolae: a once-elusive structure gets some respect. *Sci. STKE* **5548**, 1862-1865.

Mora, R., Bonilha, V. L., Marmorstein, A., Scherer, P. E., Brown, D., Lisanti, M. P. and Rodriguez-Boulan, E. (1999). Caveolin-2 localizes to the golgi complex but redistributes to plasma membrane, caveolae, and rafts when co-expressed with caveolin-1. *J. Biol. Chem.* **274**, 25708-25717.

Murthy, K. S. and Makhlouf, G. M. (2000). Heterologous desensitization mediated by G protein-specific binding to caveolin. *J. Biol. Chem.* **39**, 30211-30219.

Navarro, A., Anand-Apte, B. and Parat, M.-O. (2004). A role for caveolae in cell migration. *FASEB J.* **18**, 1801-1811.

Nobles, M., Benians, A. and Tinker, A. (2005). Heterotrimeric G proteins precouple with G protein-coupled receptors in living cells. *Proc. Natl. Acad. Sci. USA* **102**, 18706-18711.

Oh, P. and Schnitzer, J. E. (2001). Segregation of heterotrimeric G proteins in cell surface microdomains. G(q) binds caveolin to concentrate in caveolae, whereas G(i) and G(s) target lipid rafts by default. *Mol. Biol. Cell* **12**, 685-698.

Okamoto, T., Schlegel, A., Scherer, P. E. and Lisanti, M. P. (1998). Caveolins, a family of scaffolding proteins for organizing "preassembled signaling complexes" at the plasma membrane. *J. Biol. Chem.* **273**, 5419-5422.

Ostrom, R. S. (2002). New determinants of receptor-effector coupling: trafficking and compartmentation in membrane microdomains. *Mol. Pharmacol.* **61**, 473-476.

Ostrom, R. S. and Insel, P. (2004). The evolving role of lipid rafts and caveolae in G protein-coupled receptor signaling: implications for molecular pharmacology. *Br. J. Pharmacol.* **143**, 235-245.

Ostrom, R. S., Gregorian, C., Drenan, R. M., Xiang, Y., Regan, J. W. and Insel, P. A. (2001). Receptor number and caveolar co-localization determine receptor coupling efficiency to adenylyl cyclase. *J. Biol. Chem.* **276**, 42063-42069.

Parton, R. G. and Simons, K. (2007). The multiple faces of caveolae. *Nat. Rev. Mol. Cell Biol.* **8**, 185-194.

Patterson, G. H., Piston, D. W. and Barisas, B. G. (2000). Forster distances between green fluorescent protein pairs. *Anal. Biochem.* **284**, 438-440.

Pelkmans, L. and Helenious, A. (2002). Endocytosis via caveolae. *Traffic* **3**, 311-320.

Pelkmans, L., Puntener, D. and Helenius, A. (2002). Local actin polymerization and dynamin recruitment in SV40-induced internalization of caveolae. *Science* **296**, 535-539.

Philip, F. and Scarlata, S. (2004). Influence of membrane components in the binding of G proteins to membrane surfaces. *Biochemistry* **43**, 11691-11700.

Philip, F. and Scarlata, S. (2006). Real time measurements of protein affinities on membrane surfaces by fluorescence spectroscopy. *Sci. STKE*, 15-25.

Philip, F., Sengupta, P. and Scarlata, S. (2007). Signaling through a G protein coupled receptor and its corresponding G protein follows a stoichometrically limited model. *J. Biol. Chem.* **282**, 19203-19216.

Quitterer, U. and Lohse, M. J. (1999). Crosstalk between Galpha i- and Galpha q-coupled receptors is mediated by Gbeta gamma exchange. *Proc. Natl. Acad. Sci. USA* **96**, 10626-10631.

Rebecchi, M. J. and Pentyala, S. N. (2000). Structure, function, and control of phosphoinositide-specific phospholipase C. *Physiol. Rev.* **80**, 1291-1335.

Rhee, S. G. (2001). Regulation of phosphoinositide-specific phospholipase C. *Annu. Rev. Biochem.* **70**, 281-312.

Runnels, L. W. and Scarlata, S. (1999). Determination of the affinities between heterotrimeric G protein subunits and their phospholipase C-β effectors. *Biochemistry* **38**, 1488-1496.

Schlegel, A., Volonte, D., Engelman, J. A., Galbiata, F., Mehta, P., Zhange, X.-L., Scherer, P. and Lisanti, M. P. (1998). Crowded little caves: structure and function of caveolae. *Cell. Signal.* **10**, 457-463.

Schnitzer, J. E., Liu, J. and Oh, P. (1995). Endothelial caveolae have the molecular transport machinery for vesicle budding, docking, and fusion including VAMP, NSF, SNAP, annexins and GTPases. *J. Biol. Chem.* **270**, 14399-14404.

Sengupta, P., Balaji, J. and Maiti, S. (2002). Measuring diffusion in cell membranes by fluorescence correlation spectroscopy. *Methods* **27**, 374-387.

Smart, E., Ying, Y.-S., Mineo, C. and Anderson, R. G. W. (1995). A detergent-free method for purifying caveolae membrane from tissue culture cells. *Proc. Natl. Acad. Sci. USA* **92**, 10104-10108.

Smrcka, A. V. and Sternweis, P. C. (1993). Regulation of purified subtypes of phosphatidylinositol-specific phospholipase C beta by G protein alpha and beta gamma subunits. *J. Biol. Chem.* **268**, 9667-9674.

Stan, R. V., Roberts, W. G., Predescu, D., Ihida, K., Saucan, L., Ghitescu, L. and Palade, G. E. (1997). Immunoisolation and partial characterization of endothelial plasmalemmal vesicles (caveolae). *Mol. Biol. Cell* **8**, 595-605.

Strock, J. and Diversé-Pierluissi, M. A. (2004). Ca2+ channels as integrators of G protein-mediated signaling in neurons. *Mol. Pharmacol.* **66**, 1071-1076.

Tobin, A. B. (1997). Phosphorylation of phospholipase C-coupled receptors *Pharmacol. Ther.* **75**, 135-151.

Wang, L., Connelly, M. A., Ostermeyer, A. G., Chen, H. H., Williams, D. L. and Brown, D. A. (2003). Caveolin-1 does not affect SR-BI-mediated cholesterol efflux or selective uptake of cholesteryl ester in two cell lines. *J. Lipid Res.* **44**, 807-815.

Wickman, K. D. and Clapham, D. E. (1995). G-protein regulation of ion channels. *Curr. Opin. Neurobiol.* **5**, 278-285.

Xia, Z. and Liu, Y. (2001). Reliable and global measurement of fluorescence resonance energy transfer using fluorescence microscopes. *Biophys. J.* **81**, 2395-2402.